 SDHM, vol.4, no.1, pp.29-45, 2008

Energy Absorption of Thin-walled Corrugated Crash Box in Axial Crushing

H. Ghasemnejad[1], H. Hadavinia[1,2], D. Marchant[1] and A. Aboutorabi[1]

Abstract: In this paper the crashworthiness capabilities of thin-walled corrugated crash boxes in axial crushing relative to flat sidewall boxes from the same material are investigated. In order to achieve this, various design of corrugated aluminium alloy 6060 temper T4 crash boxes were chosen and their axial crushing behaviour under impact loading was studied by developing a theoretical model based on *Super Folding Element* theory and by conducting finite element analysis using LS-DYNA in ANSYS. From the theoretical and FE analysis the crush force efficiency, the specific energy absorption and the frequency and amplitude of fluctuation of the dynamic crush force of the corrugated crash boxes were calculated and the results were compared with the reference uncorrugated model. It was shown that the corrugated crash boxes have advantages of a lower initial collapse force, a lower crush force fluctuation frequency and amplitude relative to a flat sidewall box.

Keyword: Crashworthiness; Corrugation; Impact; Aluminium; Theoretical analysis

Nomenclature

A	mean area
C	width of extrusion
CFE	crush force efficiency
d	depth of corrugates
D, q	material constants in Cowper-Symonds equation
$\hat{E}$	specific energy absorption
F	force
$F_{\max}$	initial maximum collapse force
F_{md}	mean dynamic force
H	wall thickness
L	free length of specimen
m	mass of specimen
M_0	fully plastic bending moment
N	number of corrugations
SE	stroke efficiency
U_m	membrane energy
U_b	bending energy
V	impact velocity
w	crush distance
ν	Poisson's ratio
σ_0	flow stress
σ_y	yield stress
σ_u	ultimate tensile strength
δ	magnitude of trigger
δ_0	amplitude of trigger
ρ	density
λ	half pitch distance
κ	effective crush distance

[1] Faculty of Engineering, Kingston University, SW15 3DW, UK

[2] Corresponding Author. Email: h.hadavinia@kingston.ac.uk (H. Hadavinia), Tel: +44 20 8547 8864 Fax: +44 20 8547 7992

1 Introduction

The optimization technique plays an important role in the crashworthiness design of automotive structures. The use of a suitable geometrical shape and material could give great payoffs such as a lower weight, higher stiffness and a more stable energy absorption process [Alkolose et al (2003)]. Crashworthiness is defined as the ability of a restraint system or component to withstand forces below a certain level and to reduce the damage caused in those cases involving excessive dynamic forces [Mahdi et al (2006)]. For the automotive designers, it is a challenge to find an optimum design to maximise the safety. McGregor *et al*. [McGregor et al (1993)] have stated the principal stages involved in the design process of an impact member as shown in Figure 1. Based on this design philosophy, initially a preliminary geometry for the crash box is chosen, and then three

performance aspects for good crashworthiness designs practice, i.e. the collapse mode, average collapse force and maximum collapse force, are evaluated. The preliminary geometry can then be modified to enhance the performance of the crash box and the cycle of the design will be repeated until the optimum design is obtained.

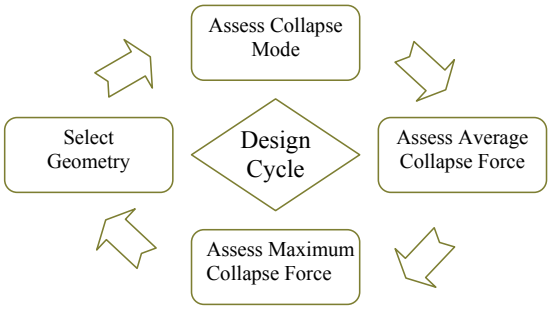

Figure 1: Design cycle for impact members [McGregor et al (1993)].

The first modern studies on the dynamic inelastic behaviour of structures commenced about fifty years ago with the introduction of the rigid-plastic idealisation [Jones (2003)]. Nowadays, car manufacturers use numerical simulations to study the crash behaviour of various vehicle structures. By using numerical modelling, not only the numbers of prototypes testing are reduced but also the numerical simulations enable new design and materials to be evaluated without extensive and expensive testing. These modelling also provide a benchmark platform for evaluating the new knowledge gained through experiments and improvements in the theories of materials and structures [Langseth et al (1999)]. The majority of the research and developments relating to crash zone are to do with energy absorption by the frontal and bending deformation of the metal structure [Transportation Research Board and National Research Council (1996)]. In principal, an efficient crashworthy design system should be able to: (i) absorb the impact kinetic energy in a controlled manner, (ii) after an impact, a sufficient survival space remain for the occupants, and (iii) the forces and accelerations experienced by the occupants in the vehicle are minimised and remain at a survival level. The total energy absorption depends on the governing deformation phenomena of all constituent parts of the structure such as thin-walled tubes, cones, frames and sections [Yamakazi and Han (2000); Singace (1997) Mahdi et al (2003); Abosbaia et al (2003)].

The structural crashworthiness requirement is generally met by the use of crumple zones. These zones exist in the front and rear of the car and protect the passenger safety cell. In a crash, these crumple zones absorb the vast majority of the crash energy through plastic collapse. Jones [Jones (1993)] has shown that an ideal energy absorber should be lightweight and maintain the maximum allowable retarding force throughout the greatest possible crush displacement while keeping the resulting axial crushing forces fluctuation frequency and amplitude relatively low. Singace and El-Sobky [Singace and El-Sobky (1997)] studied the energy absorption characteristics of axially crushed corrugated metal tube. They found that, for a controlled behaviour of an energy absorption device, corrugated tubes would be a favourable choice. Seitzberger *et al*. [Seitzberger et al (2000)] have concluded that the lower mean force for tubular member will be advantageous.

In this paper various corrugated aluminium alloy 6060 tempered T4 energy absorber square boxes were designed and their effect on the crushing behaviour and crashworthiness were studied by developing a theoretical model based on *Super Folding Element* theory and by finite element software LS-DYNA in ANSYS [Ghasemnejad et al (2007); ANSYS documentation]. Parameters such as the crush force efficiency, the energy absorption, the stroke efficiency and the frequency and amplitude of the resulting axial crushing force in each crash box were obtained and the results were compared with those from a flat sidewall square crash box hereafter referred to as the *base model*.

2 Design Aspect of Crash Box

There are three important parameters for the design of crash boxes. The first is the crush force efficiency (CFE) which is defined as the ratio between the maximum initial collapse force and the mean dynamic force. An ideal absorber can

exhibit a crush force efficiency of 100% with a rectangular-shaped force-crush distance curve. It means that initial collapse force and mean force are equal but in practice the situation of a CFE parameter equal to 1 is not achievable. The mean dynamic force is a function of the impact velocity while the mass of the striker has no noticeable influence on it. The second important parameter is the stroke efficiency (SE) which is the ratio of the stroke (crushed distance) at the bottoming out to the initial length of the absorber. High ratios indicate efficient use of the material. In such cases the force-crush distance curves are cut at a point where the force starts to increase steeply, and so maximum displacement coincides with the stroke length, and the definition of this cut-off point is somewhat arbitrary. The reported stroke lengths should be regarded only as approximate values. The third parameter is specific absorbed energy ($\hat{E}$) which is the area under the force-crush distance curve divided by the mass of the specimen. Assuming that the contribution due to the elastic deformation is negligible, the absorbed energy can approximately be regarded as the energy dissipated by plastic deformation.

In an impacted box, the force-crush distance curve can be divided into three distinct regions as shown in Figure 2. In region I, the force increases rapidly and reaches a maximum ($F_{\max}$) before dropping. In region II, the force fluctuates around a mean dynamic force (F_{md}) while a series of folds form successively in the tube so that a folded zone grows progressively down the tube in a form of mushrooming failure. In region III, all lobes touch each other and the box stiffness to impacted object increases and this will cause a rapid increase in the force.

Generally, the specification of the energy absorption component is dictated by the requirement of the design e.g., the specification for the structural design of a passenger carrying rail vehicle ends by Railtrack [Railtrack Structural Requirements for Railway Group Standard (1994)] was set at a minimum energy absorption of 1 MJ over a distance not exceeding 1 m with a mean dynamic force of 3000 kN. Under these design requirements the ideal energy absorber is a rectangle with a mean dynamic force (F_{md}) less than 3000 kN over a maximum allowable crush distance which absorbs the specified impact energy as shown in Figure 2. Also in Figure 2 the crushing behaviour of three possible realistic designs are demonstrated. Case 1 design has the highest initial maximum collapse force among the others and hence it is discarded; though its F_{md} is about the ideal solution. Case 2 will absorb higher energy in the same crush distance but its mean dynamic force is higher than the ideal crush solution. Since biomedical loading caused by impact will be experienced by the vehicle occupants, a lower mean dynamic crush force is desirable as long as the energy absorption criterion is satisfied. In Case 3, initial collapse force is relatively low and the mean crush force equal to the ideal crash box which fluctuates with low amplitude around the ideal mean dynamic force. The amplitude of fluctuations in Case 3 is lower than Case 1. As Case 3 satisfies all design requirements with least minimum initial collapse force and least mean dynamic force with minimum amplitude of fluctuation about the mean force, it is the best design amongst the designs presented in Figure 2.

3 Theoretical analysis of corrugated crash box

The dynamic mean force for an uncorrugated square box for a rigid-perfectly plastic material is derived by Abramowicz and Jones [Jones (1993)] as

$$F_m = 13.05\sigma_0 H^{\frac{5}{3}} C^{\frac{1}{3}} \left\{ 1 + (0.33V/CD)^{\frac{1}{q}} \right\} \qquad (1)$$

In the above equation because of strain rate insensitivity of aluminium alloy, the strain hardening effect is taken into account by assuming the dynamic flow stress is equal to static flow stress obtained from:

$$\sigma_0 = \frac{\sigma_y + \sigma_u}{2} \qquad (2)$$

where σ_y and σ_u are yield stress, and ultimate tensile strength of the box material, respectively.

A theoretical solution method (the so called *Super Folding Element* method) for obtaining the

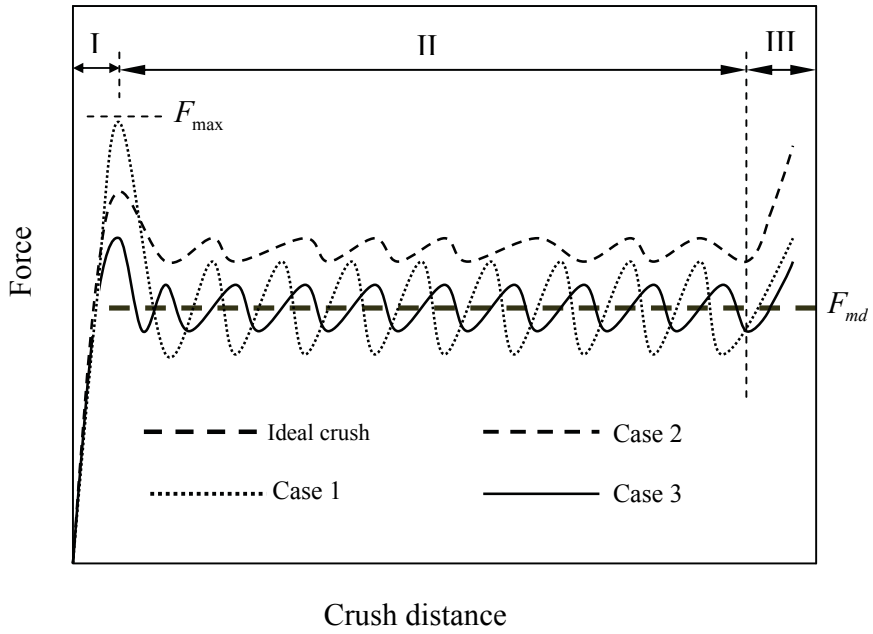

Figure 2: Comparison of different scenario of force-crush distance curve during impact.

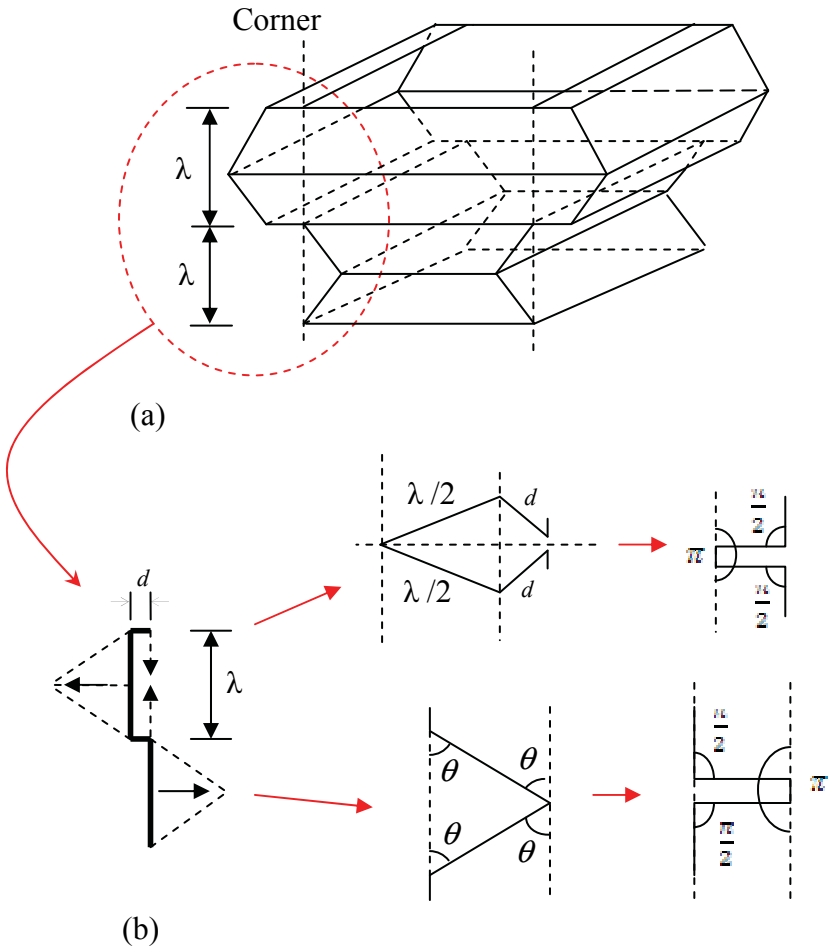

Figure 3: Presentation of dissipation in bending of a single corrugated unit with rotation angles.

mean dynamic crush force in the axial progressive crushing of thin-walled square columns was developed by Wierzbicki and Abramowicz [Wierzbicki and Abramowicz (1983)]. In this model by adopting a rigid-plastic material and using the condition of kinematic continuity on the boundaries between the rigid and deformable zones, each corner is considered having three extensional/compressional triangular elements and three stationary hinge lines. We extended this approach to the corrugated crash boxes.

From the energy balance of the system, for a complete collapse of a single fold of corrugated box, the external work done by compression of the box has to be dissipated through the rotational plastic deformation in bending and extensional/compressional deformation of the membrane walls, i.e.

$$2\lambda F_m \kappa = U_b + U_m \tag{3}$$

where λ is the corrugation pitch distance, F_m is the mean force and $\kappa \leq 1$ is a correction factor for effective crush distance. U_b and U_m are, respectively, the energy dissipation in rotational bending and extension/compression due to the membrane deformation. In the real structure, the corrugated section is never completely flattened. The effective crush distance is reported between 70-75% of the folding wavelength in previous works by Wierzbicki and Abramovicz [Wierzbicki and Abramowicz (1983)]. In the present work, by analysing the FEA results, the effective crush distance was found to vary linearly with the corrugation pitch distance as

$$\kappa = 5.3\lambda + 0.52 \tag{4}$$

i.e. as the corrugation pitch distance decreases, the effective crush distance also decreases and approach 0.52. In Eq. (4) λ is in meter.

The bending dissipated energy, U_b, was calculated by summing up the energy dissipation at stationary hinge lines. In each corrugation unit, 6 horizontal stationary hinge lines are developed, 3 at the inner and 3 at the outer circumference (Figure 3a), hence

$$U_b = \left(\sum_{i=1}^{3} M_0 \theta_i L_c\right)_{\text{extruded hinge line}} + \left(\sum_{i=1}^{3} M_0 \theta_i L_c\right)_{\text{recessed hinge line}} \tag{5}$$

where $M_0 = 2\int_0^{H/2} \sigma_0 t\,dt = \sigma_0 H^2/4$ is the fully plastic bending moment of the flange and θ is the rotation angle at each hinge line. For simplicity, it was assumed that the flanges are completely flattened after the axial compression of 2λ (Figure 3b). In this situation, the rotational angles at the hinge lines are $\pi/2$, π and $\pi/2$, respectively. The Eq. (5) for dissipated energy in bending will simplify to,

$$U_b = M_0 (2\pi L_{C1} + 2\pi L_{C2}) \tag{6}$$

whereL_{C1} and L_{C2} are the inner and outer circumference of the corrugation.

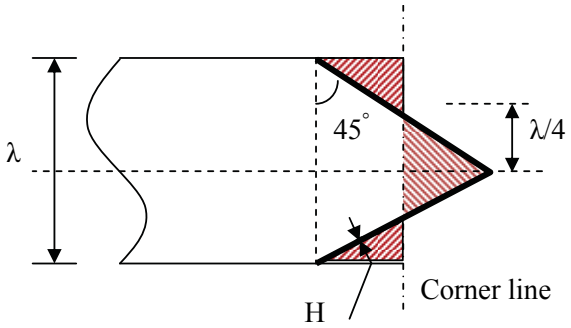

Figure 4: Presentation of the membrane energy dissipation in compression and extension.

The membrane dissipated energy, U_m, during one wavelength crushing in corner part was evaluated by integrating the extensional and compressional areas as shown in Figure 4,

$$U_m = \int_S \sigma_0 H\, dS = \sigma_0 H N_C \left(\frac{1}{2}\times\frac{\lambda}{4}\times\frac{\lambda}{4}\right)\times 8\times 2 = \frac{\sigma_0 H \lambda^2 N_C}{2} \tag{7}$$

where N_C is the number of corners. For a square corrugated unit N_C =4.

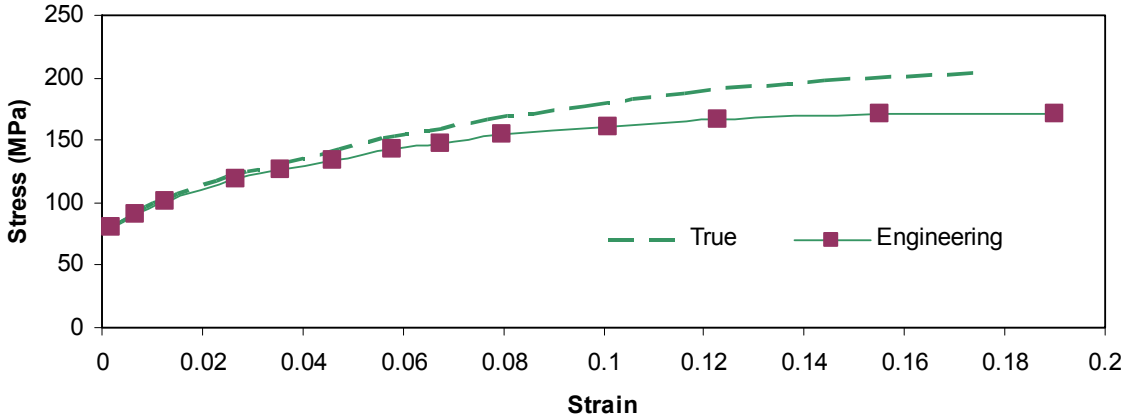

Figure 5: Stress-strain curves for AA6060-T4.

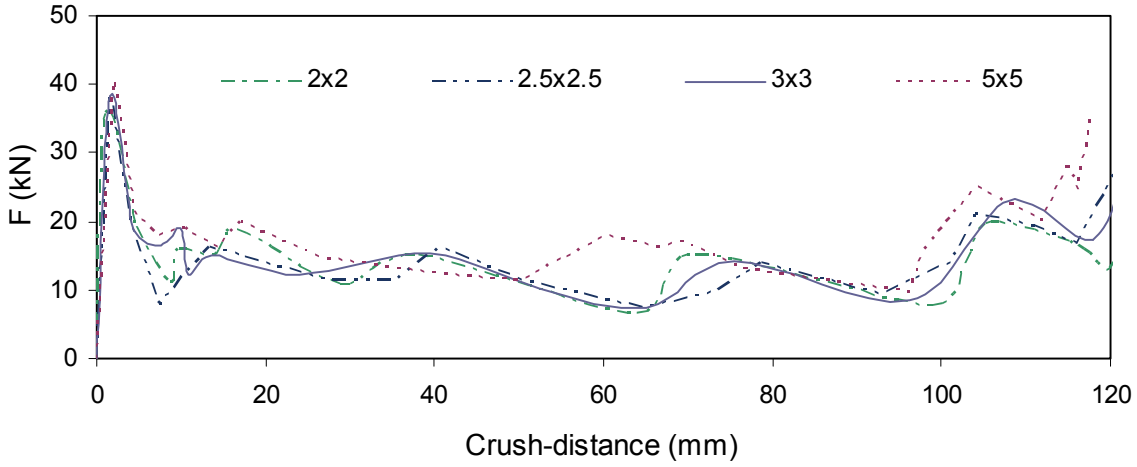

(a)

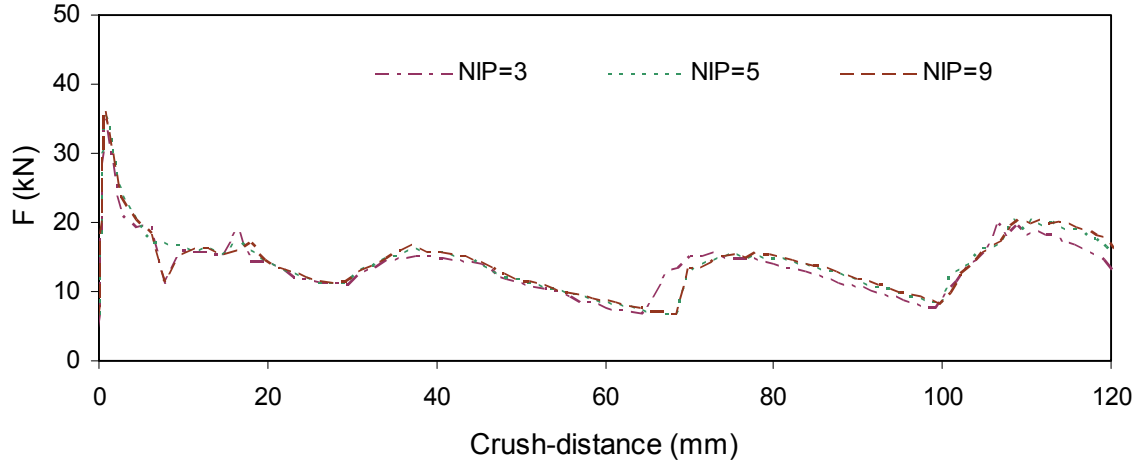

(b)

Figure 6: Effect of (a) element sizes and (b) number of integration point on the force-crush distance behaviour.

By substituting Eqs. (6) and (7) in Eq. (3), the mean force is,

$$\kappa F_m = \frac{\pi}{4}\frac{\sigma_0 H^2}{\lambda}(L_{C1}+L_{C2}) + \frac{\sigma_0 H \lambda N_C}{4} \tag{8}$$

The mean force can be obtained by substituting κ from Eq. (4) in Eq. (8).

The static mean force obtained from Eq. (8) needs to be corrected to take into account the dynamics effect. This has been done according to the ratio between dynamic and static progressive buckling forces suggested by Jones [Jones (1993)],

$$\frac{F_{md}}{F_{ms}} = \left(1+\left(\frac{0.33V}{CD}\right)^{\frac{1}{q}}\right) \tag{9}$$

The calculated dynamic mean forces obtained from the above theoretical solution for all the models are presented in Table 1. The discrepancy between the theoretical results and FE results are less than 3%.

4 Finite element studies

Nonlinear explicit finite element code ANSYS/LS-DYNA was used to model the axial crushing of the thin-walled aluminium crash boxes. These energy absorbers were modelled by the Belystchko-Lin-Tsay quadrilateral four-node thin shell elements [Belytschko et al (1984)]. These shell elements are available in the element library of LS-DYNA. The Belystchko-Lin-Tsay shell element is based on a combined co-rotational and velocity-strain formulation [Hallquist (1998)]. To simulate the quasi-static condition, the constant velocity was applied to the rigid striker. The real crushing speed is too slow for the numerical simulation. The explicit time integration method is only conditionally stable, and therefore by using real crushing speed, very small time increments was required to use. For satisfying quasi-static condition, the total kinetic energy has to be very small compared to the total internal energy over the period of the crushing process and also the crushing force-displacement response must be independent from the applied velocity.

4.1 Material modelling

In the present work, the crash boxes are made from aluminium alloy with a Young's modulus of 68.2 GPa, a yield stress of 80 MPa and a Poisson's ratio 0.3. The stress-strain relation of this material is shown in Figure 3. The advantage of using aluminium in vehicle structure is reducing the weight of the vehicle. It has been reported that savings in the load-bearing structure of an aluminium vehicle can be as much as 40–50% when compared to steel. Aluminium alloys have approximately 1/3 the weight and 1/3 the elasticity modulus of steel, and usually a lower strength. As an example, an aluminium section with a 50% thicker wall relative to the same steel section have the same stiffness but a lower weight [Meguid et al (2004)].

In LS-DYNA the aluminium was modelled by a type 24 material which is defined as MATERIAL_PIECEWISE_LINEAR_PLASTICITY, pertaining to the von Mises yield condition with isotropic strain hardening, and strain rate-dependent dynamic yield stress based on the Cowper and Symonds model. The aluminium alloy is known to be insensitive to high strain rates and therefore strain rate effect was not applied [Jones (2003)].

4.2 Sensitivity analysis of FE model

The sensitivity of the FE results to variation of element size, trigger position and the number of integration points (NIP) through the thickness was studied to find the optimum values of these parameters.

The effect of element sizes was studied by modelling the base model using 2×2, 2.5×2.5, 3×3 and 5×5mm meshes. The trigger position was located at $C/8$ (10mm from the top end of box) and the NIP through the thickness was kept 3. The results of force-crush distance of these models are compared in Figure 6a. The results show that apart from 5×5mm coarse mesh, for the finer meshes from 2×2 to 3×3mm the results are very similar and insensitive to element size.

Next the effect of NIP through the thickness was studied on a model with element size of 2×2mm and the same trigger position at $C/8$. NIP through

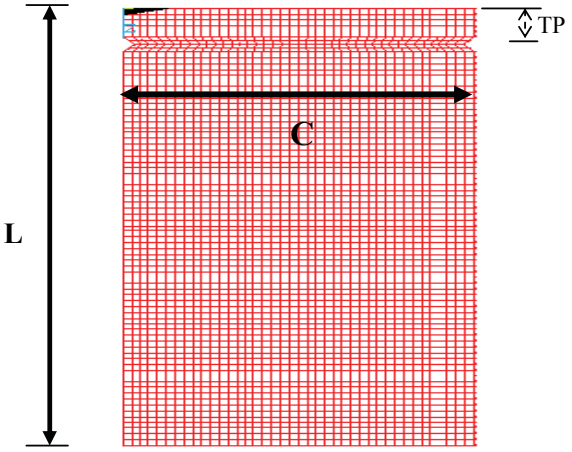

Figure 7: Trigger position (TP) in the FE model of the crash box at TP= C/16, C/8, C/4 and C/2.

the shell elements was varied at 3, 5 and 9. The results are compared in Figure 6b and they are insensitive to NIP in range of 3-9. Using higher integration points through the thickness increase the computing cost and make the structure stiffer. For further analysis NIP=3 is chosen.

The trigger position is shown in Figure 7. The effect of trigger position at $C/2$ (40mm), $C/4$ (20mm), $C/8$(10mm) and $C/16$ (5mm) from top end of box was investigated. The element size of these models was 2×2mm and the NIP was kept constant at 3. It was found that trigger position in the range of $C/8$ to $C/2$ from the top end of box has no significant effect on the response of force-crush distance diagrams, (Figure 8a). In further study, the total length of crash box was changed while keeping the element size at 2×2mm with trigger position at C/8 and NIP=3. The result shown in Figure 8b confirmed that the force-crush distance is not affected too much by the total length of crash box. In conclusion, it is found that by choosing element size between 2×2–3×3mm, trigger position between $C/8$ (10mm) and $C/2$ (40mm) and NIP of 3 will give an optimum FE parameters for modelling of crash box. In the next part of this study an element size of 3×3mm which gave lower CPU time in comparison with other element sizes, trigger position of $C/4$ (20mm) with NIP=3 were chosen.

Using these parameters in our FE models, the force-crush distance behaviour of the base model is verified by comparing to those reported in [Langseth et al (1999)] and [Zhang et al (2006)] as shown in Figure 7. The discrepancy between our base model and the results in [Langseth et al (1999)] and [Meguid et al (2004)] were minimal. There is no difference in mean dynamic force and initial maximum collapsed force between the models. Dynamic mean force obtained from the FE result was also compared with the theoretical solution given in Eq. (1). The calculated dynamic mean force from the theoretical solution is 42 kN, and from the FE analysis it is 47 kN, a difference of 9%. The FE and theoretical results are compared in Table 2.

4.3 FE modelling of corrugated crash box under impact loading

The simulation of impact, especially at high impact velocities requires very expensive equipments such as a high speed impact machine, manufacturing of specimens and a high-speed camera to detect the crushing process which takes place in fraction of a second. In this study finite element simulation is used as an alternative method to study the impact process.

A square tube under axial quasi-static or impact condition can collapse in one of these distinct crushing modes, symmetric mode, extensional mode, asymmetric mixed mode or global buckling during compression. Symmetric progressive plastic buckling is the ideal crushing mode for box like energy absorber. Extensive experimental studies [Jones (2003)] have shown that for the combination of geometrical parameters, a symmetric progressive mode of collapse of a thin-walled prismatic square column subjected to the dynamic axial loading of an AA6060 aluminium box regardless of the material temper condition observed when $32 \leq C/H \leq 44.4$. Furthermore, the localisation of the lobes for temper T4 started either at the impacted end of the specimens or at the clamped support.

Four different corrugated models were studied. In the finite element models, the free length of the crash box was chosen at 310 mm with different wall thicknesses while the total mass of all cor-

Table 1: Comparison of the dynamic mean force from theoretical results and FE analysis for corrugated crash boxes.

Model	**Wall thickness H (mm)**	**Pitch distance λ (mm)**	**Depth of corrugates, d (mm)**	W_b **(kJ)**	W_m **(kJ)**	F_{md} **(kN) FEA**	F_{md} **(kN) Theoretical**	**Error %**
1	2.49	77.5	6	5.03	23.15	39	40.9	4.9
2	2.47	51.67	6	7.43	15.31	40	38.7	-3
3	2.34	25.83	6	13.34	7.25	42	42.3	0.7
4	2.20	19.38	6	15.71	5.1	44	45	2

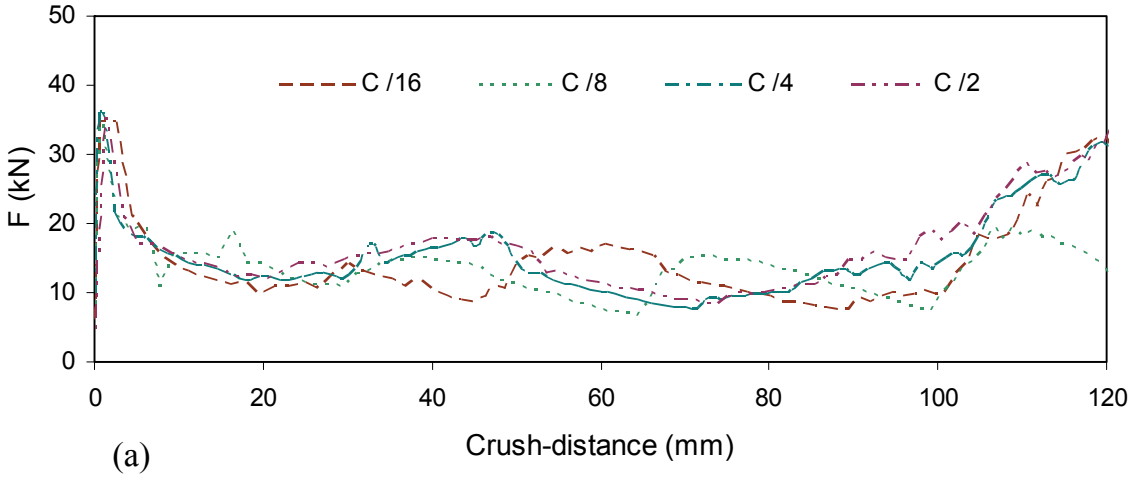

(a)

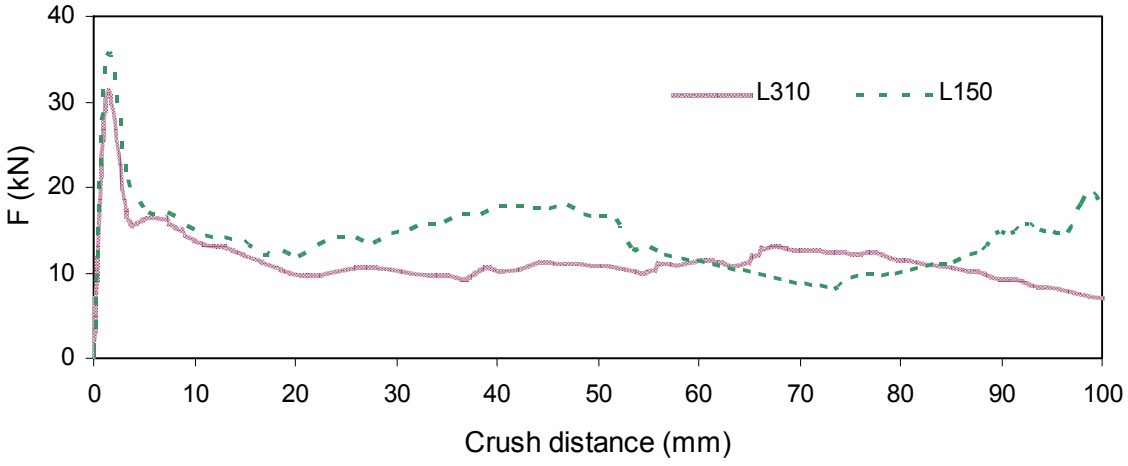

(b)

Figure 8: Effect of (a) trigger position and (b) the length of the crash box on the force-crush distance behaviour.

Table 2: Comparison of FE and analytical results of uncorrugated box under dynamic loading.

σ_0 (MPa)	C (mm)	H (mm)	$D^{(1)}$ (s^{-1})	$Q^{(1)}$	V (m/s)	F_{md} (kN) FEA	F_{md} (kN) Analytical	Error (%)
120	80	2.5	6500	4	25	40	42	5

(1) [Singace and El-Sobky (1997)]

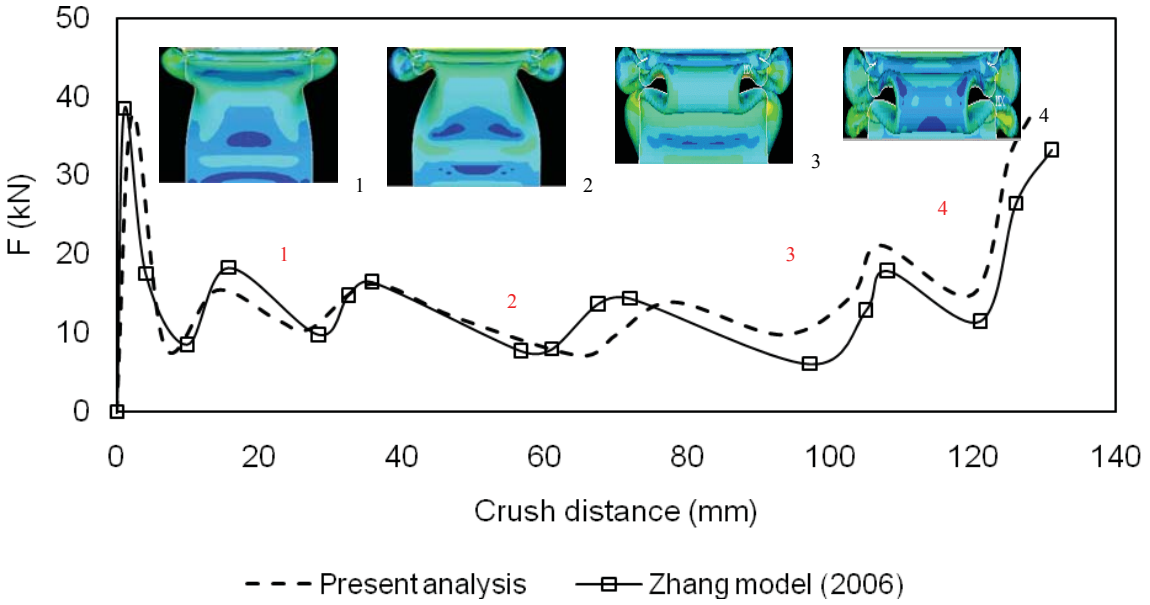

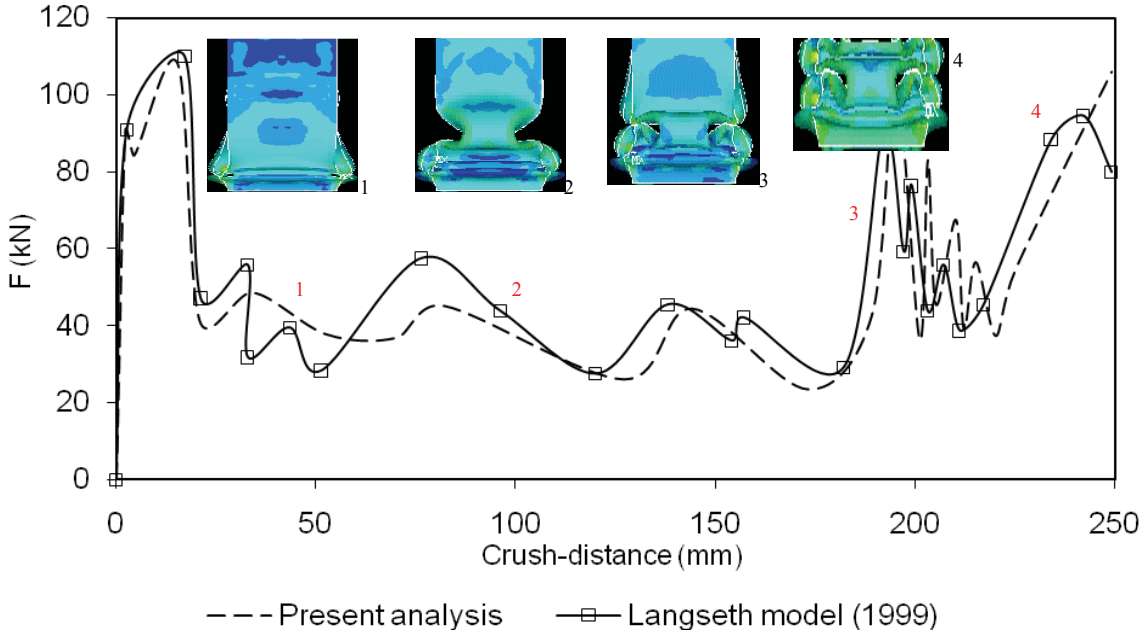

Figure 9: Comparison of force-crush distance of the base model in the present study with those in [Zhang (2006)] and [Langseth (1999)]. The inserts show von Mises stress distribution at various stages of the impact.

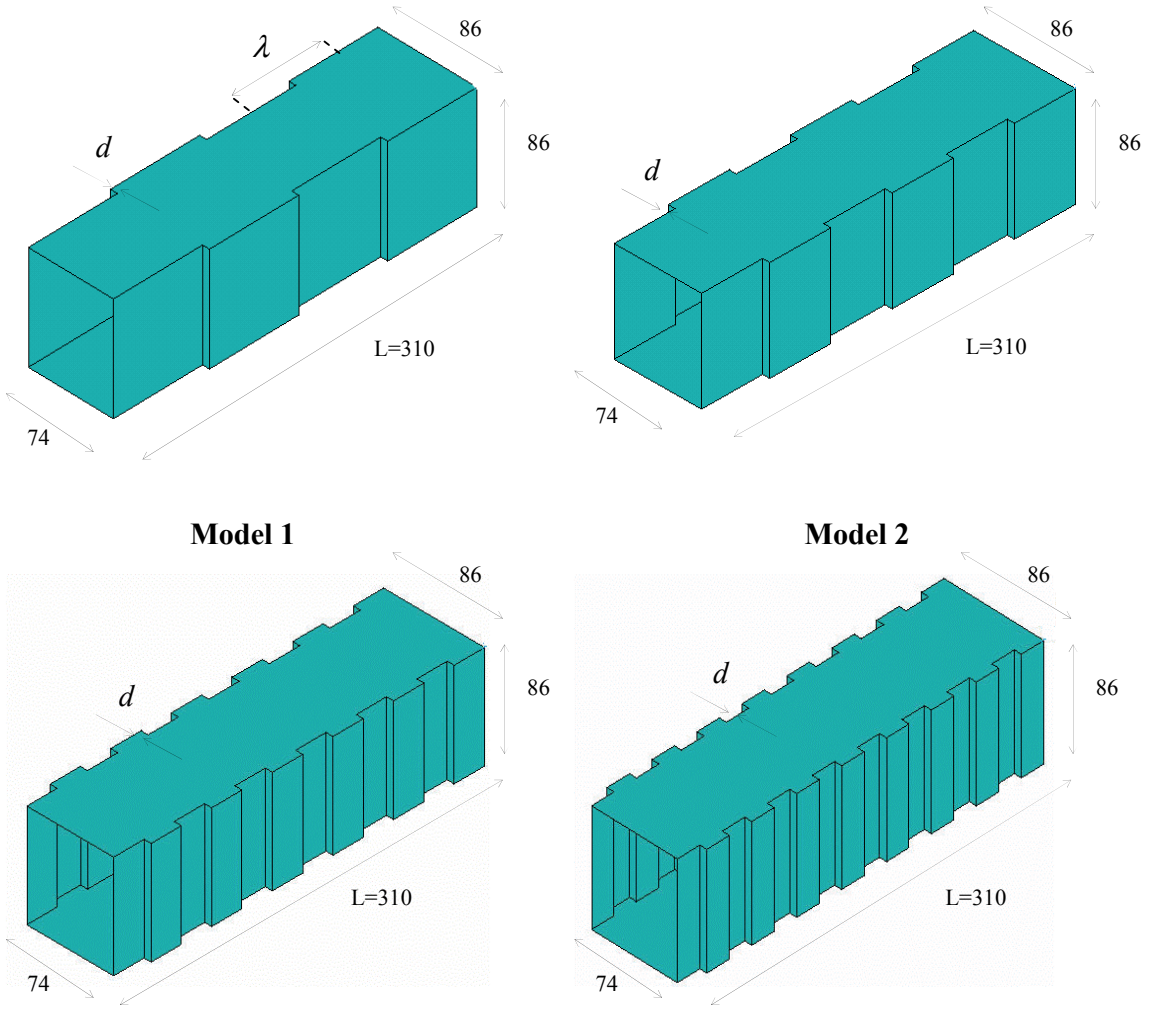

Figure 10: Isometric view of corrugated crash boxes (all dimensions in mm).

Table 3: Dimensions of the specimens.

Model	**Mean cross section (mm)**	**Wall thickness H (mm)**	**Pitch distance λ (mm)**	**Depth of corrugates, d (mm)**
1	80×86	2.49	77.5	6
2	80×86	2.47	51.67	6
3	80×86	2.34	25.83	6
4	80×86	2.20	19.38	6
Base model	80×80	2.50	N/A	-

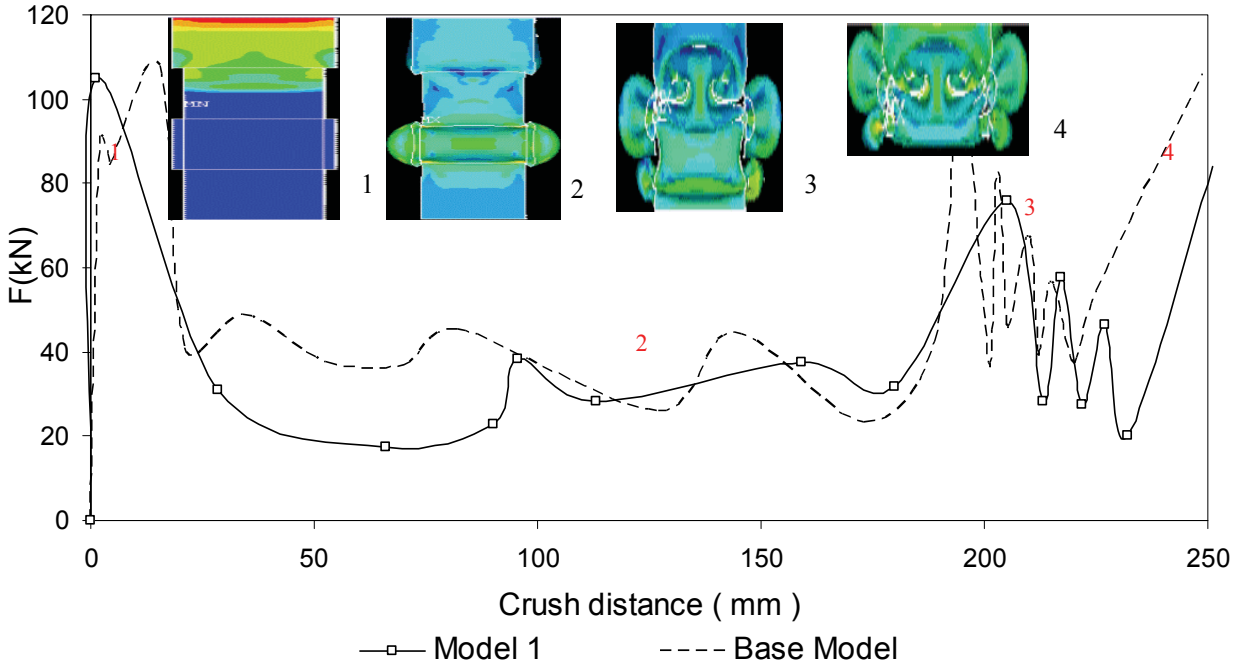

Figure 11: Force-crush distance curve in Model 1 corrugated crash box. The inserts show von Mises stress distribution at various stages.

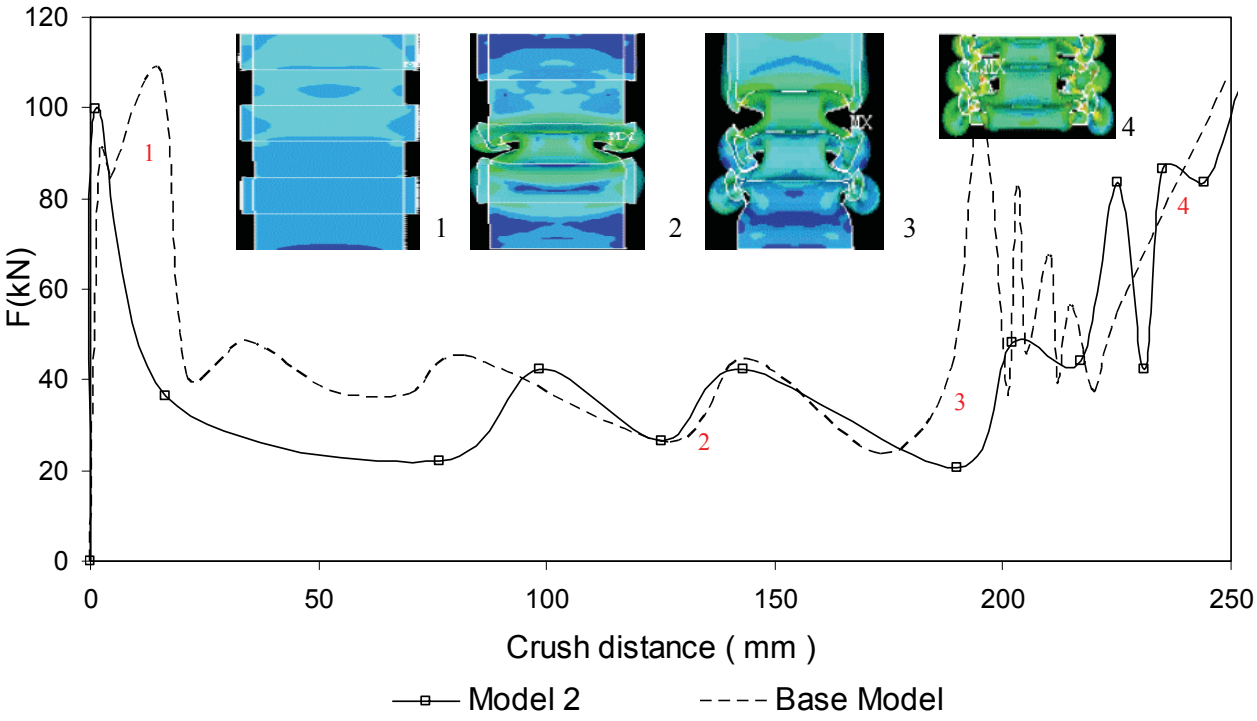

Figure 12: Force-crush distance curve in Model 2 corrugated crash box. The inserts show von Mises stress distribution at various stages.

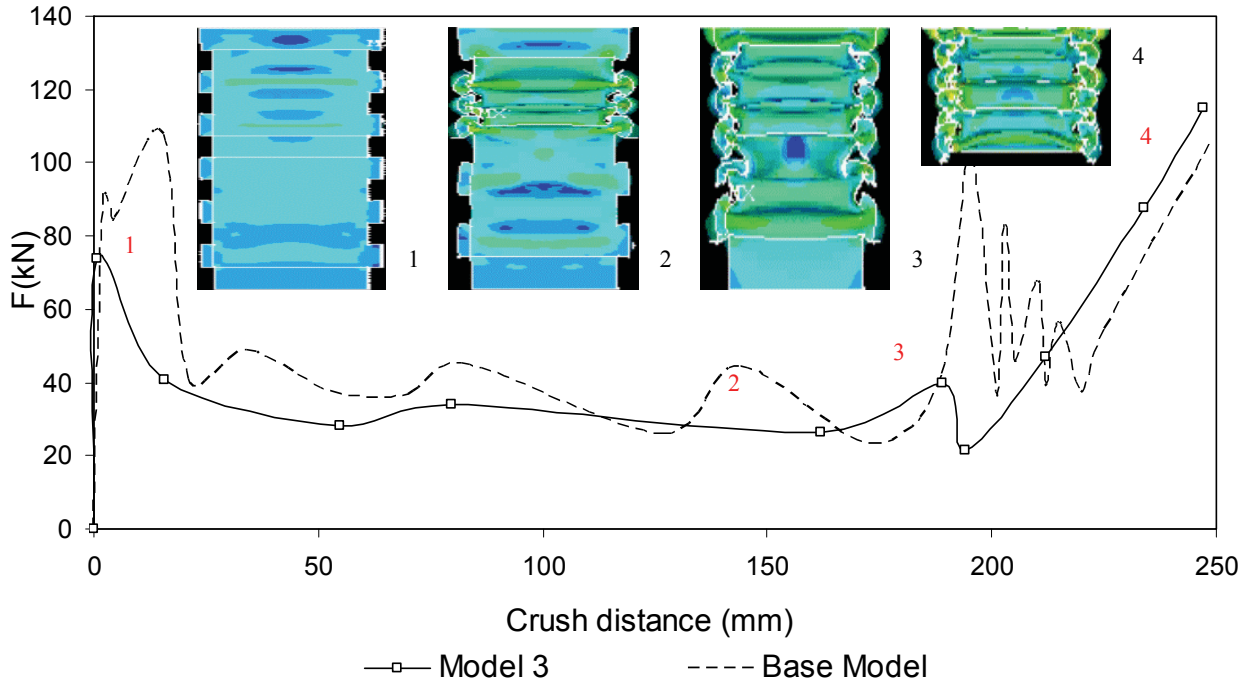

Figure 13: Force-crush distance curve in Model 3 corrugated crash box. The inserts show von Mises stress distribution at various stages.

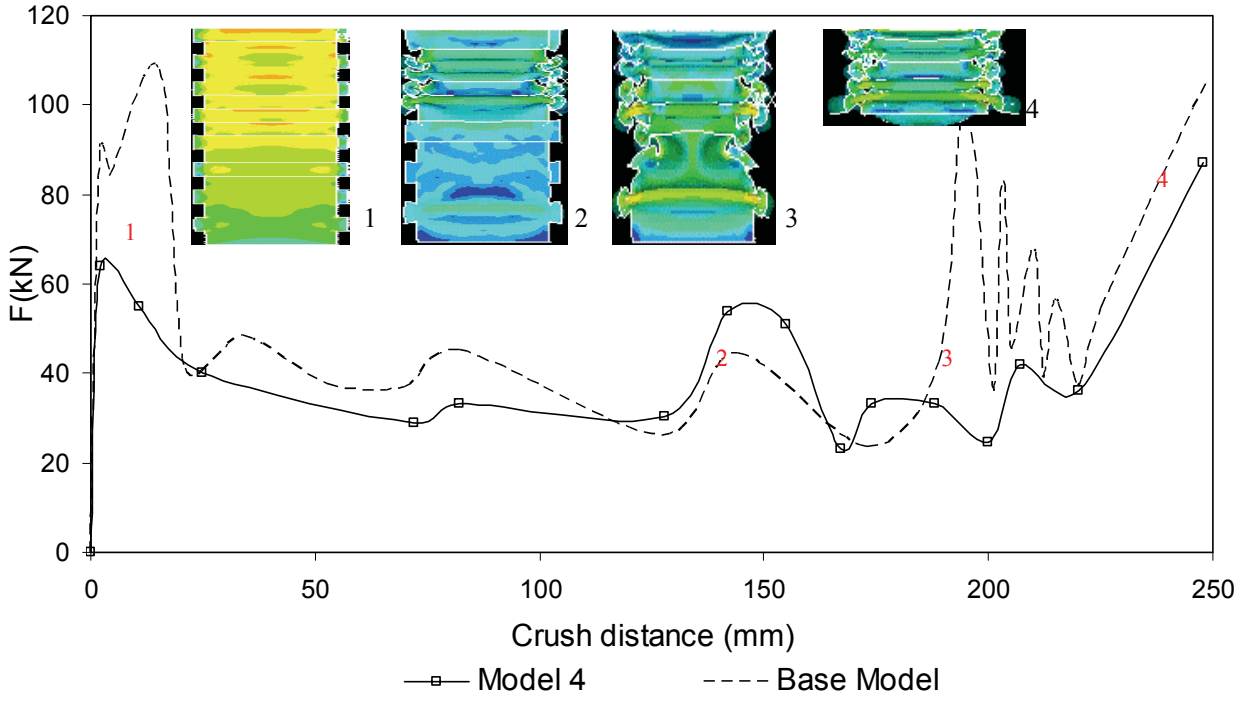

Figure 14: Force-crush distance curve in Model 4 corrugated crash box. The inserts show von Mises stress distribution at various stages.

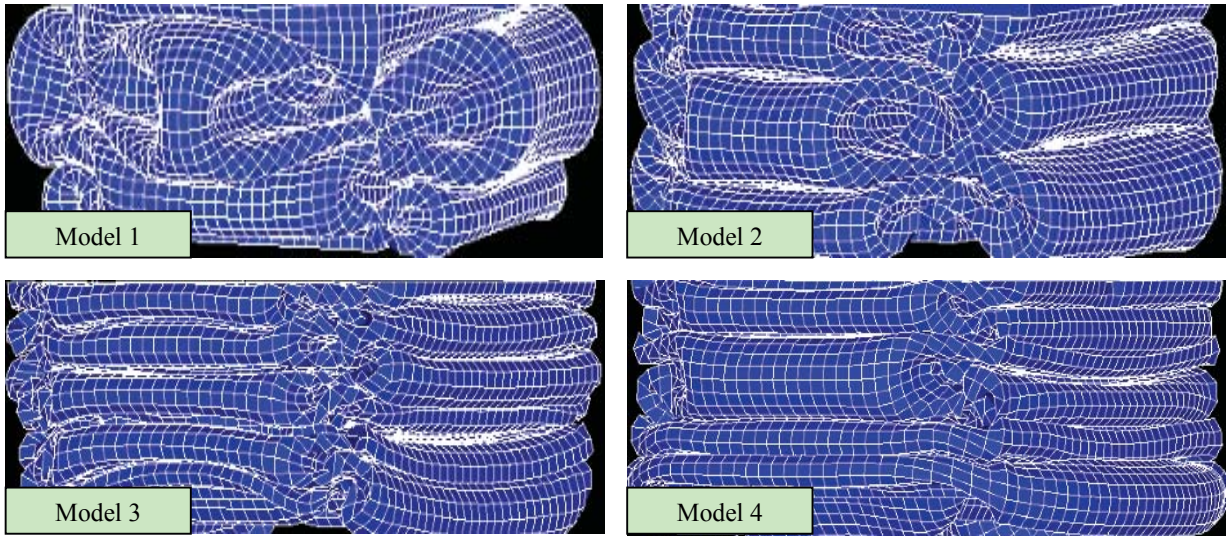

Figure 15: Symmetric collapse mode of corrugated crash boxes.

Table 4: Crashworthiness parameters of the corrugated models.

Model	$F_{\max}$ **(kN)**	F_{md} **(kN)**	**CFE %**	**SE %**	$\hat{E}$ **(kJ/kg)**
1	105	39	37	80	14.6
2	100	40	40	80	15.1
3	74	42	57	79	15.8
4	64	44	69	79	16.6
Base model	113	47	41	80	17.6

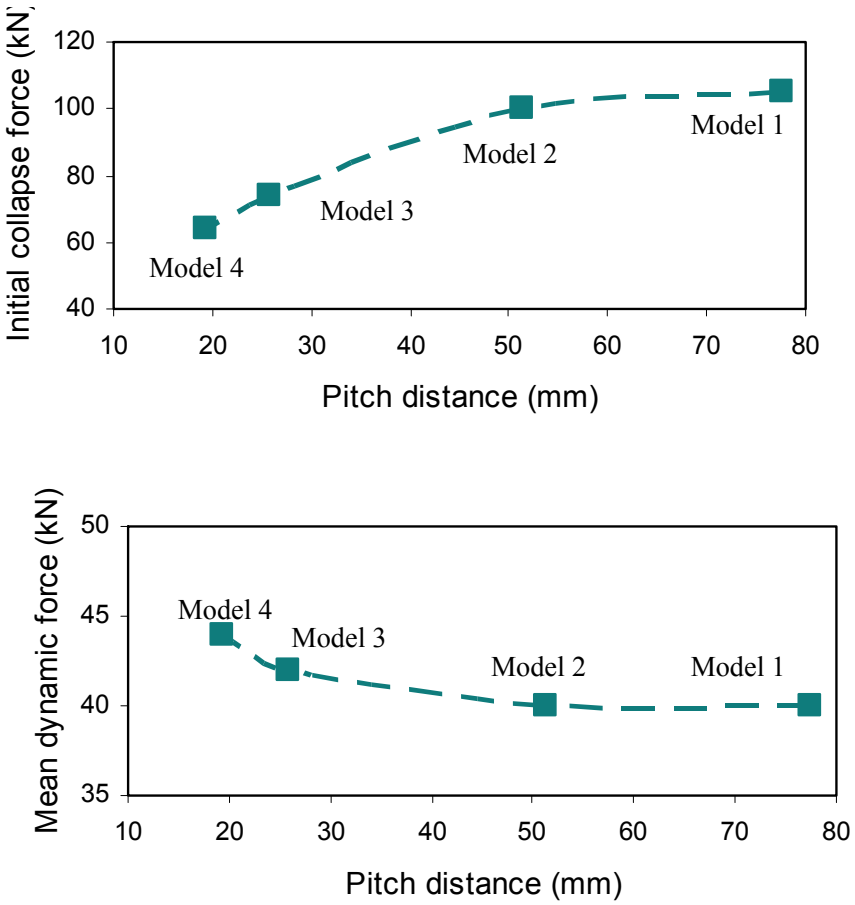

Figure 16: Variation of initial maximum collapse force ($F_{\max}$) and mean dynamic force (F_{md}) with pitch distance (λ).

rugated boxes were kept constant as in the base model, i.e. 0.664 kg. The design information for the four corrugated models and the base model are presented in Figure 10 and Table 3. The specimens were impacted at a velocity of 25 m/s with a block of 50 kg which was modelled as a rigid body. All degrees of freedom of the crash boxes were fixed at the bottom end and all the rotational degrees of freedom were fixed at the upper end to avoid unrealistic deformation modes. The contact between the striker and the specimens was modelled using a *nodes impacting surface* with a friction coefficient of 0.25 to avoid lateral movements. To account for the contact between the lobes during deformation, a *single surface* contact algorithm without friction was used. This contact algorithm is used to prevent the penetration of the deformed box boundary by its own nodes. In accordance with the mesh sensitivity studies in previous part, an element size of 3×3 was found to be a suitable size which gave satisfactory results. In the base model, a trigger mechanism with sine-wave formulation [Langseth et al (1999)] was inserted on the sidewalls of the specimen at 130mm from the end of the box to initiate the symmetric deformation mode.

5 Results and discussion

The effects of corrugations on the crushing behaviour of crash boxes were investigated by extracting the force-crush distance behaviour from FEA for each model. The force-crush distance results obtained from FEA simulations for all corrugated models are shown in Figures 11-14 together with various stages of deformation of the crash box during the deformation. In these Figures the behaviour of the base model has been

shown with dash line for comparison. In all simulations, the progressive symmetric deformation mode was found for all specimens at impact as shown in Figure 15. The FEA results show that by decreasing the corrugation pitch distance, the initial maximum collapse force ($F_{\max}$) decreases from 113 kN in the base model to 64 kN in model 4 while at the same time the mean dynamic force (F_{md}) of all corrugated models was increased in comparison with the base model (see Table 4 and Figure 16). As discussed earlier the initial collapse force is an important parameter for crashworthiness design. This gives an indication of the required force to initiate collapse and the beginning of the energy absorption process. The net results of changes in the mean dynamic force (F_{md}) and the initial maximum collapse force ($F_{\max}$) will be observed in the CFE parameter. A maximum CFE of about 70% has been achieved for model 4 as compared to 41% in the base model (see Table 4). Model 3 and 4 both have higher CFE than the base model while CFE in models 1 and 2 are slightly lower than the base model. By increasing the number of corrugations, the frequency and amplitude of the mean crush force was also decreased, and this is another advantage of corrugating a crash box. However, the stroke efficiency (SE) in all corrugated models remained nearly the same as in the base model. As explained earlier, this was related to our assumption for cut-off point in the force-crush distance diagrams. These trends are in accordance with guidelines for optimum and efficient crashworthiness designs. The summary of the results for all the models are presented in Table 4.

6 Conclusions

In this paper, the effect of corrugating the sidewall of aluminium crash box with various pitch distance on dynamic impact loading is investigated. It is shown that the dynamic crushing of corrugated aluminium boxes is affected by the corrugated pitch. By decreasing the pitch distance (λ), the initial collapse force decreases, and the energy absorption process is started at a lower maximum force compared to the base model. Also the crush force efficiencies (CFE) increases significantly as the corrugation pitch distance decreases while by decreasing the pitch distance, i.e. increasing the number of corrugations, the frequency and amplitude of mean forces are reduced. Decreasing the pitch distance (λ) has minor effect on the specific energy absorption. For all the models a progressive symmetric deformation mode is found.

In summary, corrugated crash boxes have the advantages of a lower initial collapse force, hence much higher crush force efficiency. They also have a lower crush force fluctuation frequency and amplitude relative to a flat sidewall box making them a more efficient design for automotive application.

References

Abosbaia, A.S.; Mahdi, E.; Hamuda, A.M.S.; Sahari, B.B. (2003): Axial quasi-static crushing behaviour of segmented composite tubes. *Int Jnl Compos Struct* 60(3):327-43.

Alkolose, O.; Mahdi, E.; Hamouda, A.M.S. (2003): Axial crushing of composite elliptical tubes between flat plates. *Int Jnl appl comp* 10:6339-63.

ANSYS documentation. Version 10.0, ANSYS LS-DYNA user's guide.

Belytschko, T.; Lin, J.; Tsay, C.S. (1984): Explicit algorithms for nonlinear dynamics of shells. *Comp. Meth. Appl. Mech. Eng.* 42:225-251.

Ghasemnejad, H.; Hadavinia, H.; Simpson, G.B. (2007): Crashworthiness Optimization of Automotive Structure. *Key Engineering Materials*, 348-349:661-664.

Hallquist, J.O. (1998): LS-DYNA theoretical manual. Livermore Software Technology Corporation.

Jones, N. (1993): Structural impact. Cambridge University Press, Cambridge, UK.

Jones, N. (2003): Several Phenomena in Structural Impact and Structural Crashworthiness. *European Journal of Mechanics A/Solids* 22:693-707.

Langseth, M.; Hopperstad, O.S.; Berstad, T. (1999): Crashworthiness of aluminium extrusion: validation of numerical simulation, effect of mass ratio and impact velocity. *Int. Jnl of Impact Engng* 22:829-854.

Mahdi, E.; Sahari, B.B.; Hamuda, A.M.S.; Khalid, Y.A. (2003): Experimental quasi-static axial crushing of cone-tube-cone composite system. *Int Jnl Compos Part B* 34(3):285-302.

Mahdi, E.; Mokhtar, A.S.; Asari, N.A.; Elfaki, F.; Abdullah, E.J. (2006): Nonlinear finite element analysis of axially crushed cotton fibre composite corrugated tubes. *Composite Structures* 75:39-48.

McGregor, L.J.; Meadows, D.J.; Scott, C.E.; Seeds, A.D. (1993): Impact performance of aluminium structures. In: Jones N and Wierzbicki T, Structural Crashworthiness and Failure, Elsevier Science Publisher, 385-421.

Meguid, S.A.; Stranart, J.C.; Heyerman, J. (2004): On The Layered Micromechanical Three-dimensional Finite Element Modelling of Foam-filled Columns. *Finite Element in Analysis and Design* 40:1035-1057.

Railtrack Structural Requirements for Railway Group Standard (1994): GM/RT 2100.

Seitzberger, M.; Rammerstorfer, F.G.; Gradinger, R.; Degischer, H.P.; Blaimschein, M.; Walch, C. (2000): Experimental studies on the quasi-static axial crushing of steel columns filled with aluminium foam. *Int Jnl of Sol and Struc* 37:4125-4147.

Singace, A.A. (1997): Axial crushing analysis of tubes deforming in the multi lobe mode. *Int Jnl Mech Sci* 41:865-90.

Singace, A.A.; El-Sobky, H. (1997): Behaviour of axially crushed corrugated tubes. *Int Jnl Mech Sci* 39(3):249-268.

Transportation Research Board; National Research Council (1996): Shopping for Safety: Providing Consumers Automotive Safety Information. National Academy Press.

Wierzbicki, T.; Abramowicz, W. (1983): On the crushing mechanics of thin-walled structures. *J Appl Mech Trans ASME* 50(4a):727-34.

Yamakazi, K.; Han, J. (2000): Maximization of the crushing energy absorption of cylindrical shells. *Adv Engng Software* 31:425-34.

Zhang, X.; Cheng, G.D.; Zhang, H. (2006): Theoretical prediction and numerical simulation of multi-cell square thin-walled structures. *Thin-walled structures* 44:1185-1191.